# Pose-Invariant Physiological Face Recognition in the Thermal Infrared Spectrum

P. Buddharaju
Dept. of Computer Science
University of Houston
braju@cs.uh.edu

I. T. Pavlidis
Dept. of Computer Science
University of Houston
ipavlidi@central.uh.edu

P. Tsiamyrtzis
Dept. of Statistics
Athens University of Economics
pt@aueb.gr

## Abstract

*We present a novel framework for face recognition based on physiological information. The motivation behind this effort is to capitalize on the permanency of innate characteristics that are under the skin. To establish feasibility, we propose a specific methodology to capture facial physiological patterns using the bioheat information contained in thermal imagery. First, the algorithm delineates the human face from the background using the Bayesian framework. Then, it localizes the superficial blood vessel network using image morphology. The extracted vascular network produces contour shapes that are characteristic to each individual. The branching points of the skeletonized vascular network are referred to as Thermal Minutia Points (TMP) and constitute the feature database. To render the method robust to facial pose variations we collect for each subject to be stored in the database five (5) different pose images (center, mid-left profile, left profile, mid-right profile, and right profile). During the classification stage, the algorithm first estimates the pose of the test image. Then, it matches the local and global TMP structures extracted from the test image with those of the corresponding pose images in the database. We have conducted experiments on a sizeable database of thermal facial images collected in our lab. The good experimental results show that the proposed methodology has merit. More important, the results demonstrate the feasibility of the physiological framework in face recognition and open the way for further methodological and experimental research in the area.*

## 1. Introduction

Biometrics has received a lot of attention during the last few years both from the academic and business communities. It has emerged as a preferred alternative to traditional forms of identification, like card IDs, which are not embedded into one's physical characteristics. Research into several biometric modalities including face, fingerprint, iris, and retina recognition has produced varying degrees of success [1]. Face recognition stands as the most appealing modality, since it is the natural mode of identification among humans and is totally unobtrusive. At the same time, however, it is one of the most challenging modalities [2]. Research into face recognition has been biased towards the visible spectrum for a variety of reasons. Among those is the availability and low cost of visible band cameras and the undeniable fact that face recognition is one of the primary activities of the human visual system. Machine recognition of human faces, however, has proven more problematic than the seemingly effortless face recognition performed by humans. The major culprit is light variability, which is prevalent in the visible spectrum due to the reflective nature of incident light in this band [3].

As a solution to the aforementioned problems, researchers have started investigating the use of thermal infrared for face recognition purposes [4, 5, 6]. However, many of these research efforts in thermal face recognition use the thermal infrared band only as a way to see in the dark or reduce the deleterious effect of light variability [7, 8]. Methodologically, they do not differ very much from face recognition algorithms in the visible band and can be classified either as appearance-based [9, 10] or feature-based approaches [11, 12]. Recently, attempts have been made to fuse the visible and infrared modalities to increase the performance of face recognition [13, 14, 15].

In this paper, we present a novel approach to the problem of thermal facial recognition that realizes the full potential of the thermal infrared band. It consists of a statistical face segmentation and a physiological feature extraction algorithm tailored to thermal phenomenology. The method localizes the superficial facial vasculature. This is feasible in thermal imagery due to the convective heat effect produced by vessel blood flow. We brought to the fore the idea of extracting vascular information for face recognition in [16]. The current manuscript describes a more sophisticated methodology to achieve this.

The thermal imprint of the facial vascular network appears to be characteristic to each individual for several reasons. Although major vessels always appear in the same

general areas, their exact positions and shapes vary significantly from individual to individual. Also the thermal imprint of every vessel is defined by the thickness of the fat layer and the thermal conductivity of the skin, parameters that vary from face to face. The vascular network is appealing as a feature for one additional reason: it is under the skin and for this reason very difficult to alter. Therefore, it is a feature of high permanence.

Our method operates in two phases to achieve face recognition:

- *(i) Off-line phase:* The thermal facial images are captured by a thermal infrared camera. For each subject to be stored in the database, we record five different poses. A two-step segmentation algorithm is applied on each pose image to extract the vascular network from the face. TMPs are detected on the branching points of the vascular network and are stored in the database.

- *(ii) On-line phase:* Given a query image, TMPs of its vascular network are extracted and are matched against those of the corresponding pose images stored in the database.

In the following sections, we describe our face recognition method in detail. In Section 2, we present the feature extraction algorithm. In Section 3, we discuss our approach for vascular network matching. In Section 4, we present the experimental results and attempt a critical evaluation. We conclude our paper in Section 5.

## 2. Feature Extraction

A thermal infrared camera with good sensitivity provides the ability to directly image superficial blood vessels on the human face [17]. The pattern of the underlying blood vessels is characteristic to each individual, and the extraction of this vascular network can provide the basis for a feature vector. Our feature extraction algorithm first segments the face in the scene and then localizes the superficial vasculature.

### 2.1. Face Segmentation

Due to its physiology, a human face consists of 'hot' parts that correspond to tissue areas that are rich in vasculature and 'cold' parts that correspond to tissue areas with sparse vasculature. This casts the human face as a bimodal temperature distribution entity, which can be modeled using a mixture of two Normal distributions. Similarly, the background can be described by a bimodal temperature distribution with walls being the 'cold' objects and the upper part of the subject's body dressed in cloths being the 'hot' object. Figure 1(b) shows the temperature distributions of

the facial skin and the background from a typical infrared facial image. We approach the problem of delineating facial tissue from background using a Bayesian framework since we have apriori knowledge of the bimodal nature of the scene.

We call $\theta$ the parameter of interest, which takes two possible values (skin $s$ or background $b$) with some probability. For each pixel $x$ in the image at time $t$, we draw our inference of whether it represents skin (i.e., $\theta = s$) or background (i.e., $\theta = b$) based on the posterior distribution $p^{(t)}(\theta|x_t)$ given by:

$$p^{(t)}(\theta|x_t) = \begin{cases} p^{(t)}(s|x_t), & \text{when } \theta = s, \\ p^{(t)}(b|x_t) = 1 - p^{(t)}(s|x_t), & \text{when } \theta = b. \end{cases} \tag{1}$$

We develop the statistics only for skin, and then the statistics for the background can easily be inferred from Equation (1).

According to the Bayes' theorem:

$$p^{(t)}(s|x_t) = \frac{\pi^{(t)}(s)f(x_t|s)}{\pi^{(t)}(s)f(x_t|s) + \pi^{(t)}(b)f(x_t|b)}. \tag{2}$$

Here, $\pi^{(t)}(s)$ is the prior skin distribution and $f(x_t|s)$ is the likelihood for pixel $x$ representing skin at time $t$. In the first frame ($t = 1$) the prior distributions for skin and background are considered equiprobable:

$$\pi^{(1)}(s) = \frac{1}{2} = \pi^{(1)}(b). \tag{3}$$

For $t > 1$, the prior skin distribution $\pi^{(t)}(s)$ at time $t$ is equal to the posterior skin distribution at time $t - 1$:

$$\pi^{(t)}(s) = p^{(t-1)}(s|x_{t-1}). \tag{4}$$

The likelihood $f(x_t|s)$ of pixel $x$ representing skin at time $t \geq 1$ is given by:

$$f(x_t|s) = \sum_{i=1}^{2} w_{s_i}^{(t)} N(\mu_{s_i}^{(t)}, \sigma_{s_i}^{2(t)}), \tag{5}$$

where the mixture parameters $w_{s_i}$ (weight), $\mu_{s_i}$ (mean), $\sigma_{s_i}^2$ (variance): $i = 1, 2$ and $w_{s_2} = 1 - w_{s_1}$ of the bi-modal skin distribution can be initialized and updated using the EM algorithm. For that, we select $N$ representative facial frames (off-line) from a variety of subjects that we call the training-set. Then, we manually segment, for each of the $N$ frames, skin (and background) areas, which yields $N_s$ skin (and $N_b$ background) pixels as shown in Figure 1(a).

We apply a similar EM process for determining the initial parameters of the background distributions. Once a data point $x_t$ becomes available, we decide that it represents skin if the posterior distribution for the skin, $p^{(t)}(s|x_t) > 0.5$ and that it represents background if the posterior distribution for the background, $p^{(t)}(b|x_t) > 0.5$. Isolated
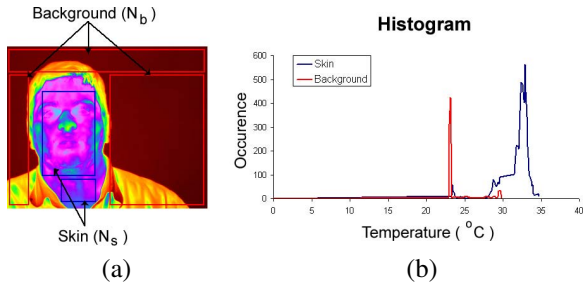
IEEE
COMPUTER
SOCIETY

Figure 1. Skin and Background: (a) Selection of samples for EM algorithm; (b) Corresponding bi-modal temperature distributions.
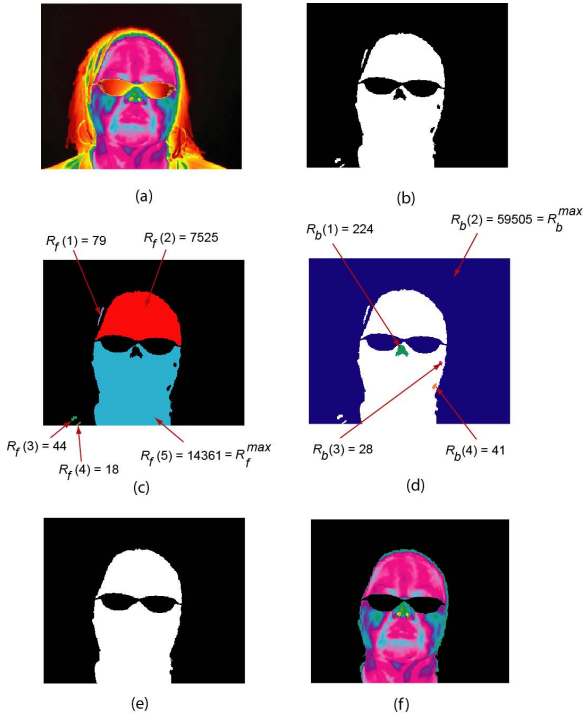


Figure 2. Segmentation of facial skin region: (a) Original thermal facial image; (b) Binary segmented image; (c) Foreground regions each represented in different color; (d) Background regions each represented in different color; (e) Binary mask after foreground and background corrections; (f) Final segmentation result after post-processing.

mislabeled patches can be easily corrected through post-processing. Figure 2 shows typical results of our face segmentation algorithm.

## 2.2. Segmentation of Superficial Blood Vessels

Once a face is delineated from the rest of the scene, the segmentation of superficial blood vessels from the facial tissue is carried out in the following two steps:

1. The image is processed to reduce noise and enhance edges.

2. Morphological operations are applied to localize the

superficial vasculature.

In thermal imagery of human tissue the major blood vessels have weak sigmoid edges, which can be handled effectively using anisotropic diffusion. The anisotropic diffusion filter is formulated as a process that enhances object boundaries by performing intra-region as opposed to inter-region smoothing. The mathematical equation for the process is:

$$\frac{\partial I(\bar{x}, t)}{\partial t} = \nabla(c(\bar{x}, t)\nabla I(\bar{x}, t)). \qquad (6)$$

In our case $I(\bar{x}, t)$ is the thermal infrared image, $\bar{x}$ refers to the spatial dimensions, and t to time. $c(\bar{x}, t)$ is called the diffusion function. The discrete version of the anisotropic diffusion filter of Equation (6) is as follows:

$$
\begin{aligned}
I_{t+1}(x, y) = I_t + \frac{1}{4} * [&c_{N,t}(x, y)\nabla I_{N,t}(x, y) \\
+ &c_{S,t}(x, y)\nabla I_{S,t}(x, y) + c_{E,t}(x, y)\nabla I_{E,t}(x, y) \\
+ &c_{W,t}(x, y)\nabla I_{W,t}(x, y)].
\end{aligned} \qquad (7)
$$

The four diffusion coefficients and four gradients in Equation (7) correspond to four directions (i.e., North, South, East, and West) with respect to the location (x,y). Each diffusion coefficient and the corresponding gradient are calculated in the same manner. For example, the coefficient along the North direction is calculated as follows:

$$c_{N,t}(x, y) = exp(\frac{-\nabla I_{N,t}^2(x, y)}{k^2}), \qquad (8)$$

where $\nabla I_{N,t} = I_t(x, y + 1) - I_t(x, y)$.

Image morphology is then applied on the diffused image to extract the blood vessels that are at a relatively low contrast compared to that of the surrounding tissue. We employ for this purpose a top hat segmentation method, which is a combination of erosion and dilation operations. Top hat segmentation takes two forms. First form is the white top hat segmentation that enhances the bright objects in the image, while the second one is the black top hat segmentation that enhances dark objects. In our case, we are interested in the white top hat segmentation because it helps with enhancing the bright ('hot') ridge like structures corresponding to the blood vessels. In this method the original image is first opened and then this opened image is subtracted from the original image as shown below:

$$
\begin{aligned}
I_{open} &= (I \ominus S) \oplus S, \\
I_{top} &= I - I_{open},
\end{aligned} \qquad (9)
$$

where $I$, $I_{open}$, $I_{top}$ are the original, opened, and white top hat segmented images respectively, S is the structuring element, and $\ominus$, $\oplus$ are morphological erosion and dilation operations respectively. Figure 3(b) depicts the result of applying anisotropic diffusion to the segmented facial tissue shown in Figure 3(a). Figure 3(c) shows the corresponding blood vessels extracted using white top hat segmentation.
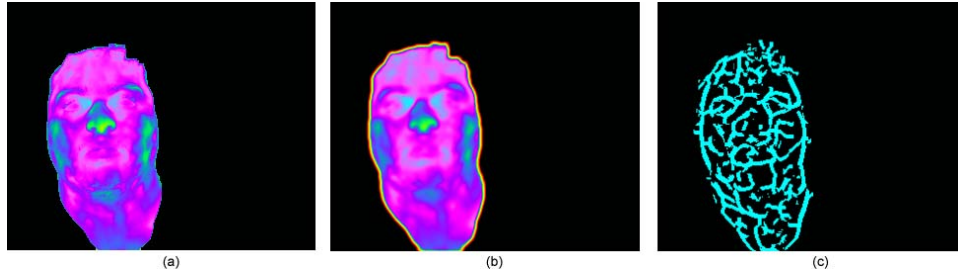
Figure 3. Vascular network extraction: (a) Original segmented image; (b) Anisotropically diffused image; (c) Blood vessels extracted using white top hat segmentation.
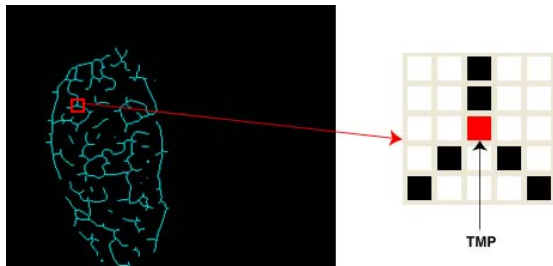


Figure 4. Thermal Minutia Point (TMP) extracted from the thinned vascular network.



Figure 5. Spurious TMPs: (a) Clustered TMPs; (b) Spike formed due to a short branch.

### 2.3. Extraction of TMPs

The extracted blood vessels exhibit different contour shapes between subjects. We call the branching points of the blood vessels Thermal Minutia Points (TMPs). TMPs can be extracted from the blood vessel network in ways similar to those used for fingerprint minutia extraction. A number of methods have been proposed [18] for robust and efficient extraction of minutia from fingerprint images. Most of these approaches describe each minutia point by at least three attributes, including its type, its location in the fingerprint image, and the local ridge orientation. We adopt a similar approach for extracting TMPs from vascular networks. Our methodology consists of the following steps:

1. The local orientation of the vascular network is estimated.

2. The vascular network is skeletonized.

3. The TMPs are extracted from the thinned vascular network.

4. The spurious TMPs are removed.

Local orientation $\Psi(x, y)$ is the angle formed at $(x, y)$ between the blood vessel and the horizontal axis. Estimating the orientation field at each pixel provides the basis for capturing the overall pattern of the vascular network. We use the approach proposed in [19] for computing the orientation image because it provides pixel-wise accuracy.
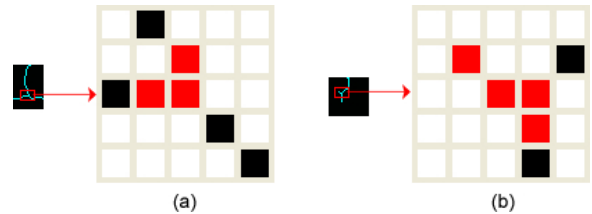
Next, the vascular network is thinned to one-pixel thickness [20]. Each pixel in the thinned map contains a value of 1 if it is on the vessel and 0 if it is not. Considering 8-neighborhood $(N_0, N_1, ..., N_7)$ around each pixel, a pixel $(x, y)$ represents a TMP if $(\sum_{i=0}^{7} N_i) > 2$ (see Figure 4).

It is desirable that the TMP extraction algorithm does not leave any spurious TMPs since this will adversely affect the matching performance. Removal of clustered TMPs (see Figure 5(a)) and spikes (see Figure 5(b)) helps to reduce the number of spurious TMPs in the thinned vascular network.

The vascular network of a typical facial image contains around 50-80 genuine TMPs whose location $(x, y)$ and orientation $(\Psi)$ are stored in the database. Figure 6 shows the results of each stage of the feature extraction algorithm on a thermal facial image.

## 3. Matching

Each subject's record in the database consists of five (5) different poses to account for pose variation during the testing phase. Since facial images from the same person look quite different across multiple views, it is very important that the search space includes facial images with pose similar to the pose of the test image. Given a test image, we first estimate its pose. Then, the task is simply to match the TMP network extracted from the test image against the TMP database corresponding to the estimated pose.

### 3.1. Estimation of Facial Pose

To the best of our knowledge, it is the first time that the issue of pose estimation in thermal facial imagery is ad-
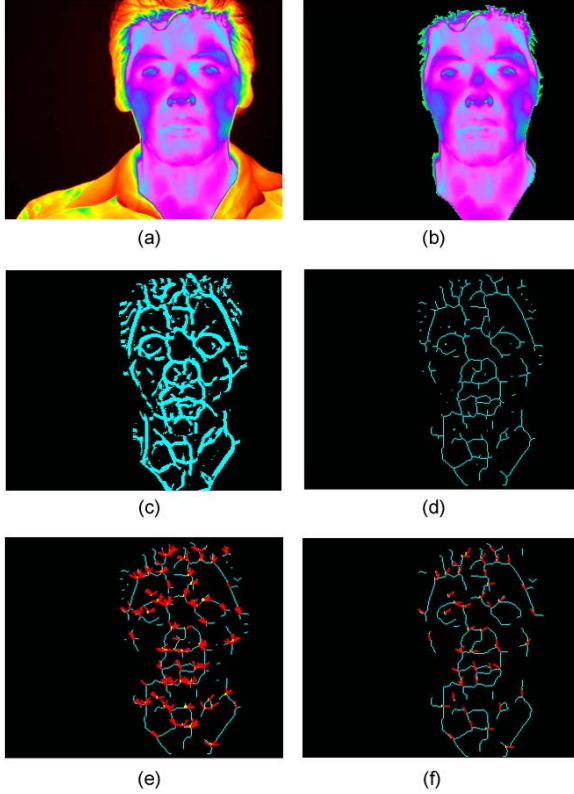
Figure 6. Visualization of the various stages of the feature extraction algorithm: (a) A typical thermal facial image; (b) Facial tissue delineated from the background; (c) Vascular network extracted from thermal facial image; (d) Thinned vessel map; (e) Extracted TMPs from branching points; (f) Spurious TMPs removed.

dressed. However, as it is the case with face recognition in general, a number of efforts have been made to address the issue of facial pose estimation in visible band imagery [21, 22]. We capitalize upon the algorithm proposed in [21] for estimating head pose across multiple views. We apply principal component analysis (PCA) on the thermal facial images in the training set to reduce the dimensionality of the training examples. Figure 7 illustrates sample face images in the database across multiple views. Then, we train the Support Vector Machine (SVM) classifier with the PCA vectors of face samples. Given a test image, SVM can classify it against one of the five poses (center, mid-left profile, left profile, mid-right profile and right profile) under consideration.

## 3.2. Matching of TMPs

Numerous methods have been proposed for matching fingerprint minutiae, most of which try to simulate the way forensic experts compare fingerprints [18]. Popular techniques are alignment-based point pattern matching, local structure matching, and global structure matching. Local minutiae matching algorithms are fast, simple, and



Figure 7. Samples from our database with five different poses; from left to right: left profile, mid-left profile, center, mid-right profile, and right profile views

more tolerant to distortions. Global minutiae matching algorithms feature high distinctiveness. A few hybrid approaches [23, 24] have been proposed where the advantages of both local and global methods are exploited. We use such a method [23] to perform TMP matching.

For each TMP $M(x, y, \Psi)$ that is extracted from the vascular network, we consider its $N$ nearest-neighbor TMPs $M(x_n, y_n, \Psi_n)$, $n = 1, ..., N$. Then, the TMP $M(x, y, \Psi)$ can be defined by a new feature vector:

$$L_M = \{\{d_1, \varphi_1, \vartheta_1\}, \{d_2, \varphi_2, \vartheta_2\}, ..., \{d_N, \varphi_N, \vartheta_N\}, \Psi\} \quad (10)$$

where

$$
\begin{aligned}
d_n &= \sqrt{(x_n - x)^2 + (y_n - y)^2} \\
\varphi_n &= diff(\Psi_n, \Psi), \ n = 1, 2, ..., N \\
\vartheta_n &= diff\left(\arctan\left(\frac{y_n - y}{x_n - x}\right), \Psi\right) \quad (11)
\end{aligned}
$$

The function $diff()$ calculates the difference of two angles and scales the result within the range $[0, 2\pi)$ [24]. Given a test image $\mathbf{I_t}$, the feature vector of each of its TMP is compared with the feature vector of each TMP of a database image. Two TMPs $M$ and $M'$ are marked to be a matched pair if the absolute difference between corresponding features is less than specific threshold values $\{\delta_d, \delta_\varphi, \delta_\vartheta, \delta_\Psi\}$. The threshold values should be chosen in such a way that they accommodate linear deformations and translations. The final matching score between the test image and a database image is given by:

$$Score = \frac{NUM_{match}}{\max(NUM_{test}, NUM_{database})} \quad (12)$$

where $NUM_{match}$ represents number of matched TMP pairs, and $NUM_{test}$, $NUM_{database}$ represent number of

IEEE
COMPUTER
SOCIETY

TMPs in test and database images respectively. If the highest matching score between the test and database images is greater than a specific threshold, the corresponding database image is classified as a match. If not, the match is considered weak and the classifier concludes that the subject does not have a record in the database.

## 4. Experimental Results

To evaluate our method, we built a dataset of thermal facial images from volunteers of different sex, race, and age groups. The dataset consists of 7590 thermal facial images from 138 subjects (55 images per subject) with varying pose and facial expressions. Five images from each subject (each image representing one of the five training poses) were used for training. From these training images we extracted TMPs and stored them in the database. The remaining 50 images per subject at arbitrary poses were used for testing.

The images were captured using a high quality Mid-Wave Infra-Red (MWIR) camera produced by Flir Systems (Phoenix model) [25]. The camera was outfitted with a $50mm$ MWIR lens also from Flir Systems.

### 4.1. Low Permanence Problem

A major challenge associated with thermal face recognition is the recognition performance over time [26]. Facial thermograms may change depending on the physical condition of the subject. This renders difficult the task of acquiring similar features for the same person over time. Previous face recognition methods in thermal infrared that use direct temperature data reported degraded performance over time [10]. However, our method attempts to solve this problem by extracting facial physiological information to build its feature space. This information is not only characteristic to each person but also remains invariant to physical conditions as shown in the example of Figure 8. In our database we have several subject images, which were captured as far as 6 months apart. Although, the thermal facial maps of the same subject appear to shift, the vascular network is invariant. In imaging terms, the contrast between the temperatures in the vascular pixels and the surrounding pixels is relatively invariant, albeit the absolute temperature values shift appreciably. This is a direct consequence of the thermoregulatory mechanism of the human body. Our morphological image processing simply capitalizes upon this phenomenon and extracts the invariant vascular contours out of the variable facial thermal maps.

### 4.2. Frontal Pose and Arbitrary Pose Experiments

Many face recognition algorithms that perform well on the frontal image datasets often have problems when tested on images with arbitrary poses [2]. Our face recognition algorithm overcomes this problem by using multiple pose
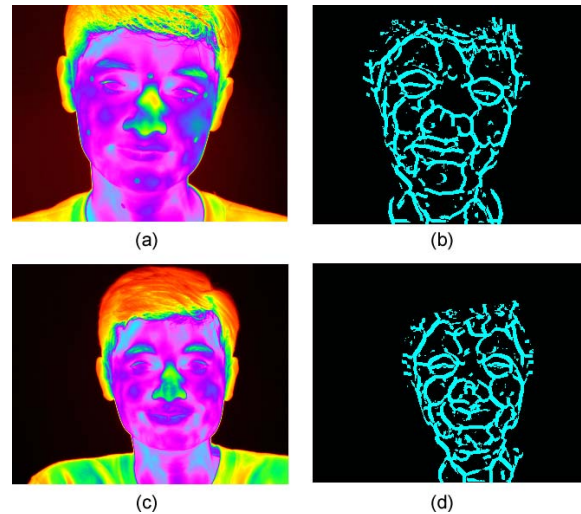


Figure 8. (a) Thermal facial image of a subject acquired on 10-17-2003 and (b) corresponding vascular network; (c) Thermal facial image of the same subject acquired on 04-29-2004 and (d) corresponding vascular network.

images for training, which allows pose invariance in the test image. We found experimentally that the five (5) poses we used for training our face recognition algorithm are sufficient to accommodate yaw rotations (including tilt rotations to a certain extent). As shown in Figure 9, when an image that is close to the mid-left profile is queried, pose estimation correctly picks the corresponding mid-left profile image from the training dataset to perform matching. The small variation in pose that exists between the query and database images might cause minor position and angle differences in the corresponding TMPs extracted from those images. This can be compensated by choosing appropriate values for thresholds $\{\delta_d, \delta_\varphi, \delta_\vartheta, \delta_\Psi\}$ discussed in section 3.2.

We conducted two experiments to evaluate the performance of our face recognition system. In the first experiment we took into account only frontal pose images. Specifically, we constrained the test set to images with poses between mid-left profile and mid-right profile. This test set was matched against frontal images in the database. This is a typical experimental procedure used for testing most of the current face recognition algorithms. In the second experiment we used the entire test set, which includes images from all five (5) poses. This test set was matched against the entire database, which contains five (5) pose images per subject. Figures 10 and 11 shows results of these two experiments. Specifically, Figure 10 shows the Cumulative Math Characteristic (CMC) curves of the two experiments, and Figure 11 shows the ROC curves based on various threshold values for the matching score discussed in Section 3.2.

First, one can observe that our face recognition method performs better in the arbitrary pose experiment rather than
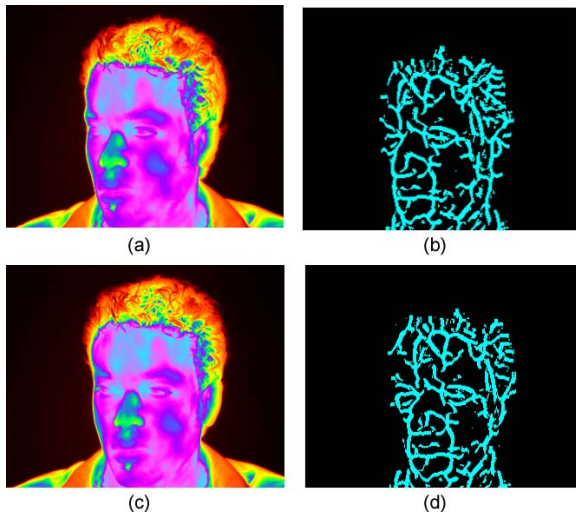
Figure 9. (a) Test image and (b) corresponding vascular network; (c) Mid-left profile image picked from training database by pose estimation and (d) corresponding vascular network.
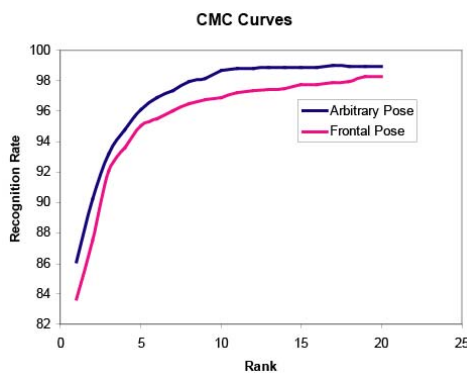


Figure 10. CMC Curve of proposed algorithm on our dataset.

the frontal pose experiment. This is to be expected as test cases close to mid-left and mid-right profile in the first experiment may be lost, since only frontal database images are being used for matching. In the second experiment, more poses are at play, but also much finer gradation of database pose images.

Second, the results demonstrate the promise as well as some problems with our methodology. The CMC curve shows that rank 1 recognition is over 86% and rank 5 recognition is over 96%. This performance puts a brand new approach close to the performance of mature visible band recognition methods. In contrast, the ROC curve reveals a weakness of the current method, as it requires false acceptance rate over 20% to reach positive acceptance rate above the 86% range. To address this problem we believe we need to pay more attention in eliminating the incorrect TMPs as well as the non-linear deformations in the extracted vascular network.
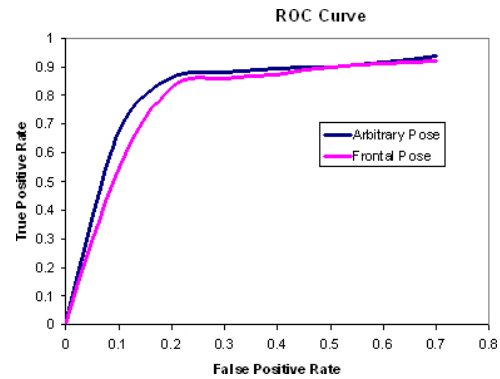


Figure 11. ROC curve of proposed algorithm on our dataset.

## 5. Conclusions and Future Work

We have outlined a novel approach to the problem of face recognition in thermal infrared. The cornerstone of the approach is the use of characteristic and time-invariant physiological information to construct the feature space.

Although, thermal facial maps shift over time, the contrast between superficial vasculature and surrounding tissue remains invariant. This physiological feature has permanence and is very difficult to be altered (under the skin). Therefore, it gives a potent advantage to any face recognition method that may use it.

We developed a method that represents an attempt to realize this physiological framework for face recognition. Our main goal was to establish the feasibility and assess the promise of the overall concept. In our method, we pay particular attention to neutralize the adverse effect of pose variability in the matching process. Our method also borrows some ideas from fingerprint recognition, since the vascular network appears to have phenomenological similarities with the ridge network.

The current method has some weak points. Specifically, it lacks a rigorous quality control mechanism when it comes to extraction of vascular contours. True, most of the contours appear to be at places where superficial vasculature is expected (e.g., carotid and temporal), but this is only a qualitative assessment. The current method also uses a crude mechanism to account for non-linearities in the deformation of the vascular network. Finally, the present method features a simplistic threshold-based classification algorithm. Our ongoing work is addressing all these issues.

It is a credit to the physiological framework, that despite the deficiencies of the current methodology, the performance is good. It is an indication that the method is aided by the natural uniqueness of the feature space.

## Acknowledgements

## References

[1] A. Jain, R. Bolle, and S. Pankanti. *Biometrics: Personal Identification in Networked Society*. Kluwer Academic Publishers, 1st edition, 1999. 1

[2] W. Zhao, R. Chellappa, P. J. Phillips, and A. Rosenfeld. Face recognition: A literature survey. *ACM Computing Surveys (CSUR)*, 35(4):399–458, December 2003. 1, 6

[3] I. Pavlidis and P. Symosek. The imaging issue in an automatic face/disguise detection system. In *Proceedings of IEEE Workshop on Computer Vision Beyond the Visible Spectrum: Methods and Applications*, pages 15–24, Hilton Head Island, South Carolina, USA, June 2000. 1

[4] F. Prokoski. History, current status, and future of infrared identification. In *Proceedings of IEEE Workshop on Computer Vision Beyond the Visible Spectrum: Methods and Applications*, pages 5–14, Hilton Head Island, South Carolina, USA, June 2000. 1

[5] D.A. Socolinsky and A. Selinger. A comparative analysis of face recognition performance with visible and thermal infrared imagery. In *Proceedings of 16th International Conference on Pattern Recognition*, volume 4, pages 217–222, Quebec, Canada, 2002. 1

[6] J. Wilder, P.J. Phillips, C. Jiang, and S. Wiener. Comparison of visible and infrared imagery for face recognition. In *Proceedings of the Second International Conference on Automatic Face and Gesture Recognition*, pages 182–187, Killington, Vermont, October 1996. 1

[7] D.A. Socolinsky, L.B. Wolff, J.D. Neuheisel, and C.K. Eveland. Illumination invariant face recognition using thermal infrared imagery. In *Proceedings of the IEEE Computer Society Conference on Computer Vision and Pattern Recognition(CVPR 2001)*, volume 1, pages 527–534, Kauai, Hawaii, United States, 2001. 1

[8] A. Selinger and D.A. Socolinsky. Face recognition in the dark. In *Proceedings of the Joint IEEE Workshop on Object Tracking and Classification Beyond the Visible Spectrum*, Washington D.C., June 2004. 1

[9] R. Cutler. Face recognition using infrared images and eigenfaces. cs.umd.edu/rgc/face/face.htm, 1996. 1

[10] X. Chen, P.J. Flynn, and K.W. Bowyer. PCA-based face recognition in infrared imagery: Baseline and comparative studies. In *Proceedings of the IEEE International Workshop on Analysis and Modeling of Faces and Gestures*, pages 127–134, Nice, France, October 17 2003. 1, 6

[11] A. Srivastava and X. Liu. Statistical hypothesis pruning for recognizing faces from infrared images. *Journal of Image and Vision Computing*, 21(7):651–661, 2003. 1

[12] P. Buddharaju, I. Pavlidis, and I. Kakadiaris. Face recognition in the thermal infrared spectrum. In *Proceedings of the Joint IEEE Workshop on Object Tracking and Classification Beyond the Visible Spectrum*, Washington D.C., June 2004. 1

[13] Jingu Heo, S.G. Kong, B.R. Abidi, and M.A. Abidi. Fusion of visual and thermal signatures with eyeglass removal for robust face recognition. In *Proceedings of the Joint IEEE Workshop on Object Tracking and Classification Beyond the Visible Spectrum*, Washington D.C., June 2004. 1

[14] A. Gyaourova, G. Bebis, and I. Pavlidis. Fusion of infrared and visible images for face recognition. In *Proceedings of the 8th European Conference on Computer Vision*, Prague, Czech Republic, May 2004. 1

[15] D.A. Socolinsky and A. Selinger. Thermal face recognition in an operational scenario. In *Proceedings of the IEEE Computer Society Conference on Computer Vision and Pattern Recognition*, volume 2, pages 1012–1019, Washington, D.C, June 2004. 1

[16] P. Buddharaju, I.T. Pavlidis, and P. Tsiamyrtzis. Physiology-based face recognition. In *Proceedings of the IEEE Advanced Video and Signal based Surveillance*, Como, Italy, September 2005. 1

[17] C. Manohar. Extraction of superficial vasculature in thermal imaging. Master's thesis, University of Houston, Houston, TX, December 2004. 2

[18] D. Maltoni, D. Maio, A.K. Jain, and S. Prabhakar. *Handbook of Fingerprint Recognition*. Springer Verlag, June 2003. 4, 5

[19] M.D. Almeida Oliveira and N.J. Leite. Reconnection of fingerprint ridges based on morphological operators and multiscale directional information. In *17th Brazilian Symposium on Computer Graphics and Image Processing*, pages 122–129, Curitiba, PR, Brazil, October 2004. 4

[20] B.K. Jang and R.T. Chin. One-pass parallel thinning: analysis, properties, and quantitative evaluation. *IEEE Transactions on Pattern Analysis and Machine Intelligence*, 14(11):1129–1140, November 1992. 4

[21] Z. Yang, H. Ai, B. Wu, S. Lao, and L. Cai. Face pose estimation and its application in video shot selection. In *Proceedings of the 17th International Conference on Pattern Recognition*, volume 1, pages 322–325, Cambridge, UK, August 2004. 5

[22] Y. Li, S. Gong, J. Sherrah, and H. Liddell. Support vector machine based multi-view face detection and recognition. *Image and Vision Computing*, 22(5):413–427, 2004. 5

[23] S. Yang and I.M. Verbauwhede. A secure fingerprint matching technique. In *Proceedings of the 2003 ACM SIGMM Workshop on Biometrics Methods and Applications*, pages 89–94, Berkley, California, 2003. 5

[24] Xudong Jiang and Wei-Yun Yau. Fingerprint minutiae matching based on the local and global structures. In *Proceedings of the 15th International Conference on Pattern Recognition*, volume 2, pages 1038–1041, Barcelona, Catalonia, Spain, September 2000. 5

[25] Flir Systems. 25 esquire road, north billerica, massachussetts 01862. http://www.flir.com. 6

[26] D.A. Socolinsky and A. Selinger. Thermal face recognition over time. In *Proceedings of the 17th International Conference on Pattern Recognition*, volume 4, pages 23–26, August 2004. 6

**IEEE COMPUTER SOCIETY**